Biochimica et Biophysica Acta 1852 (2015) 2563–2573

Contents lists available at ScienceDirect

Biochimica et Biophysica Acta

journal homepage: www.elsevier.com/locate/bbadis

Lack of cyclophilin D protects against the development of acute lung injury in endotoxemia

Fruzsina Fonai [a], Janos K. Priber [a], Peter B. Jakus [a], Nikoletta Kalman [a], Csenge Antus [a], Edit Pollak [b], Gergely Karsai [b], Laszlo Tretter [c], Balazs Sumegi [a,d,e], Balazs Veres [a,*]

[a] Department of Biochemistry and Medical Chemistry, Medical Faculty, University of Pecs, Pecs, Hungary
[b] Department of Comparative Anatomy and Developmental Biology, Faculty of Sciences, University of Pecs, Pecs, Hungary
[c] Department of Medical Biochemistry, Semmelweis University, Budapest, Hungary
[d] Szentagothai Research Center, University of Pecs, Pecs, Hungary
[e] MTA-PTE Nuclear and Mitochondrial Interactions Research Group, Pecs, Hungary

ARTICLE INFO

Article history:
Received 2 June 2015
Received in revised form 4 September 2015
Accepted 12 September 2015
Available online 15 September 2015

Keywords:
Acute lung injury
Lipopolysaccharide
Cyclophilin D
Reactive oxygen species
NF-κB

ABSTRACT

Sepsis caused by LPS is characterized by an intense systemic inflammatory response affecting the lungs, causing acute lung injury (ALI). Dysfunction of mitochondria and the role of reactive oxygen (ROS) and nitrogen species produced by mitochondria have already been proposed in the pathogenesis of sepsis; however, the exact molecular mechanism is poorly understood. Oxidative stress induces cyclophilin D (CypD)-dependent mitochondrial permeability transition (mPT), leading to organ failure in sepsis. In previous studies mPT was inhibited by cyclosporine A which, beside CypD, inhibits cyclophilin A, B, C and calcineurin, regulating cell death and inflammatory pathways. The immunomodulatory side effects of cyclosporine A make it unfavorable in inflammatory model systems. To avoid these uncertainties in the molecular mechanism, we studied endotoxemia-induced ALI in CypD$^{-/-}$ mice providing unambiguous data for the pathological role of CypD-dependent mPT in ALI. Our key finding is that the loss of this essential protein improves survival rate and it can intensely ameliorate endotoxin-induced lung injury through attenuated proinflammatory cytokine release, down-regulation of redox sensitive cellular pathways such as MAPKs, Akt, and NF-κB and reducing the production of ROS. Functional inhibition of NF-κB was confirmed by decreased expression of NF-κB-mediated proinflammatory genes. We demonstrated that impaired mPT due to the lack of CypD reduces the severity of endotoxemia-induced lung injury suggesting that CypD specific inhibitors might have a great therapeutic potential in sepsis-induced organ failure. Our data highlight a previously unknown regulatory function of mitochondria during inflammatory response.

© 2015 Published by Elsevier B.V.

1. Introduction

Sepsis is a severe systemic inflammatory process caused by bacterial agents, such as lipopolysaccharide (LPS). LPS plays a crucial role in the induction of inflammatory responses and acute lung injury (ALI), leading to acute respiratory distress syndrome (ARDS) [1,2]. The binding of LPS to toll-like receptor (TLR) 4 initiates signaling pathways, culminating in the activation of mitogen-activated protein kinases (MAPK) and NF-κB [3,4]. As a consequence of NF-κB activation, the expression of cytokines and chemokines is up-regulated, causing neutrophil infiltration into the lung [5,6,7]. Leukocytes produce reactive oxygen species (ROS) and nitrogen monoxide (NO), in order to eliminate pathogens. However, the excessive production of these reactive agents can damage cellular components and lead to epithelial and endothelial cell death and tissue damage. LPS-induced ROS can further enhance the activity of redox-sensitive inflammatory transcription factors and signaling kinases such as MAPKs and Akt [8–11].

Cytosolic Ca^{2+} overload or ROS can trigger the opening of mitochondrial permeability transition (mPT) pore leading to the collapse of ATP production, release of proapoptotic molecules and initiating further ROS production. Cyclophilin D (CypD), a matrix peptidyl-prolyl cis-trans-isomerase, encoded by the nuclear Ppif gene, is a modulator of mPT although the exact molecular composition of the pore is still under debate [12,13]. Studies with mitochondria lacking CypD demonstrated very low Ca^{2+}-sensitivity and delayed mPT pore opening, clearly favoring an indispensable modulatory role of CypD [14,15,13]. The generally used inhibitor of mPT is cyclosporine A (CsA) [16] which inhibits, not only CypD, but also cyclophilin A, B, C and calcineurin, therefore has a wide range of signaling effects — including inflammatory

* Corresponding author at: Department of Biochemistry and Medical Chemistry, University of Pecs Medical School, 12 Szigeti str., H-7624 Pecs, Hungary.
E-mail address: balazs.veres@aok.pte.hu (B. Veres).

http://dx.doi.org/10.1016/j.bbadis.2015.09.004
0925-4439/© 2015 Published by Elsevier B.V.

signaling — unrelated to CypD [17–20]. Thus, immunomodulatory effects of CsA make it unfavorable for investigating the role of mPT under inflammatory conditions. The role of mPT has been implicated in many pathological conditions accompanied by oxidative damage; however, there are only a few studies regarding the role of mPT in inflammatory processes, and no experiment has been conducted to date to evaluate its participation in ALI. Here, we give the first specific evidence for the role of CypD-dependent mPT in ALI using CypD knock-out mice.

2. Materials and methods

2.1. Ethics statement

Animal experiments were performed according to Hungarian Governmental Regulation 40/2013. (II. 14.) in accordance to the Directive 2010/63/EU of the European Parliament and of the Council on the protection of animals used for scientific purposes. The license was approved by the County Governmental Office (No. BA02/2000–20/2011) lasting for five years (2013–2017).

2.2. Animals

Male C57BL/6 mice were from Charles River Hungary Breeding and genetically engineered homozygous male Ppif−/− cyclophilin D knock-out mice with C57BL/6 background were supplied by Prof. László Tretter (Semmelweis University, Budapest, Hungary). The mice were kept under standard conditions.

2.3. Materials

LPS from Escherichia coli 0127:B8 and all materials that are not specified elsewhere were purchased from Sigma-Aldrich (St. Louis, MO). Anti-phospho-p44/42, anti-p44/42, anti-phospho-Akt, anti-Akt, anti-phospho-p38, anti-p38, anti-phospho-JNK, anti-JNK, anti-phospho-NF-κB p65, anti-NF-κB p65, anti-phospho-IκBα and anti-IκBα primary antibodies for immunoblotting were from Cell Signaling Technology (Danvers, MA), anti-MKP-1, anti-4-hydroxy-2-noneal Michael adducts, anti-nitrotyrosine and anti-GAPDH antibodies were from Millipore (Billerica, MA).

2.4. ALI model and survival study

To induce murine endotoxemia, intraperitoneal LPS (40 mg/kg, dissolved in PBS) was given, control groups received PBS (10 μl/g). Primarily survival study was performed with age-matched wild type (n = 8) and CypD knock-out mice. Mice were monitored for clinical signs of endotoxemia and lethality every hour for 96 h, after that they were monitored 3 times a day till the end of the first week. No late deaths were observed in any of the experimental groups. Alternatively, 24 h after treatment the mice were anesthetized with isoflurane (Isopharma). Lungs were removed, and processed as follows: the right upper lobe was fixed in 10% paraformaldehyde, except for a piece which was put into primary fixative (2% paraformaldehyde/2% glutaraldehyde) for electronmicroscopy; the right lower lobes were snap frozen in liquid N_2; the left upper lobe was put into RNAlater RNA stabilization reagent (Qiagen, Hilden, Germany); the left lower lobe lung homogenate was prepared as described later.

2.5. Western blot analysis

10 mg of frozen tissue was homogenized (50 mM TRIS, 50 mM EDTA, 50 mM sodium metavanadate, 0.5% protease inhibitor cocktail, 0.5% phosphatase inhibitor cocktail, pH = 7.4) and the protein concentration was determined with a DC™ Protein Assay kit (Bio-Rad, Hercules, CA). Western blotting was performed as described previously [9]. Peroxidase labeling was visualized with the Pierce ECL Western blotting Substrate (Thermo Scientific, Waltham, MA) detection system. Quantification of band intensities of the blots was performed by ImageJ software.

2.6. Cytokine determination by ELISA from lung homogenate

After removal of the left lower lobe, the tissue was rinsed in ice-cold PBS and homogenized. Protein concentration was determined with DC™ Protein Assay kit (Bio-Rad). TNFα, IL-1β and IL-10 concentrations were measured with ELISA Ready-SET-Go! (eBioscience, San Diego, CA): 200 μg protein/well was used, the cytokine-amount was expressed in optical density at 450 nm.

2.7. mRNA isolation from lung tissue and quantitative RT-PCR

RNA was isolated from tissue samples kept in RNALater (Qiagen) solution using TRIzol reagent (Invitrogen, Grand Island, NY). Total RNA concentration was determined using spectrophotometric method (IMPLEN NanoPhotometer™, München, Germany) and reverse-transcribed into cDNA with MMLV RT/RevertAid™ First Strand cDNA Synthesis Kit (Fermentas, Burlington, Canada). RT-PCR was performed with 1 μl of cDNA in MiniOpticon Real-Time PCR System (Bio-Rad) using SYBR Green Supermix kit (Bio-Rad). Specific primers against CD14, IL-1α, Cxcl2, IFN-γ, iNOS, TNFα and actin were used. The relative gene expression was calculated with ΔΔCt method using BIO-RAD CFX Manager software.

2.8. Pulmonary histopathology

The paraformaldehyde fixed superior lobe of the right lung was embedded in paraffin and cut into 5 μm sections. Hematoxylin-eosin staining was performed using standard protocol. Slides were scored in a double blinded manner by an independent expert using the scoring system described previously [21]. Five slides in each group were assessed under high power field and evaluated for intra-alveolar and interstitial neutrophil accumulation, presence of proteinaceous debris and hyaline membrane, and also alveolar wall thickening.

2.9. Immunohistochemistry

The lung tissue sections were probed with antibodies against 4-hydroxy-2-noneal Michael adducts and nitrotyrosine. Formalin-fixed, paraffin-embedded 5 μm tissue sections were deparaffinized

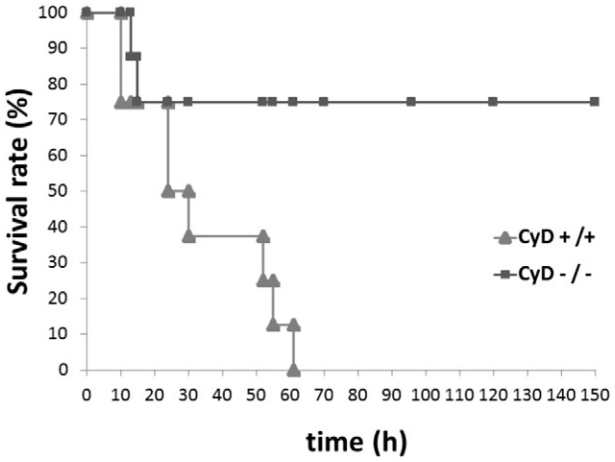

Fig. 1. Mice lacking CypD survive lethal endotoxemia. Survival study was carried out with age-matched wild-type (n = 8) and CypD knock-out mice (n = 8). Survival was monitored for 7 days, after 40 mg/kg intraperitoneal LPS administration.

and rehydrated followed by heat-induced epitope retrieval using 97 °C heat exposure for 20 min. Sections were incubated in primary antibody over-night. Blocking and staining procedures were performed with Dako EnVision™ FLEX detection system with Dako Autostainer Plus instruments (Glostrup, Denmark). All sections were counterstained with hematoxylin.

2.10. Electron microscopy

Tissue samples were rinsed in 0.1 M phosphate buffer then fixed in 2% glutaraldehyde/2% paraformaldehyde for 3 h. After a post-fixation step (osmium tetraoxide 1% in 0.1 M phosphate buffer) samples were dehydrated and embedded into Durcupan epoxy resin. Serial ultrathin sections were cut and collected on cupper grids, then passed onto drops of uranyl acetate, later on lead citrate. Following the routine counterstaining samples were rinsed in distilled water and dried. Samples were observed and documented with JEOL 1200 (Tokyo, Japan) transmission electron microscope.

2.11. Statistical analysis

Comparisons between experimental groups were made by one-way ANOVA and post-hoc test. Data represent mean ± SEM. A value of $p < 0.05$ was considered statistically significant.

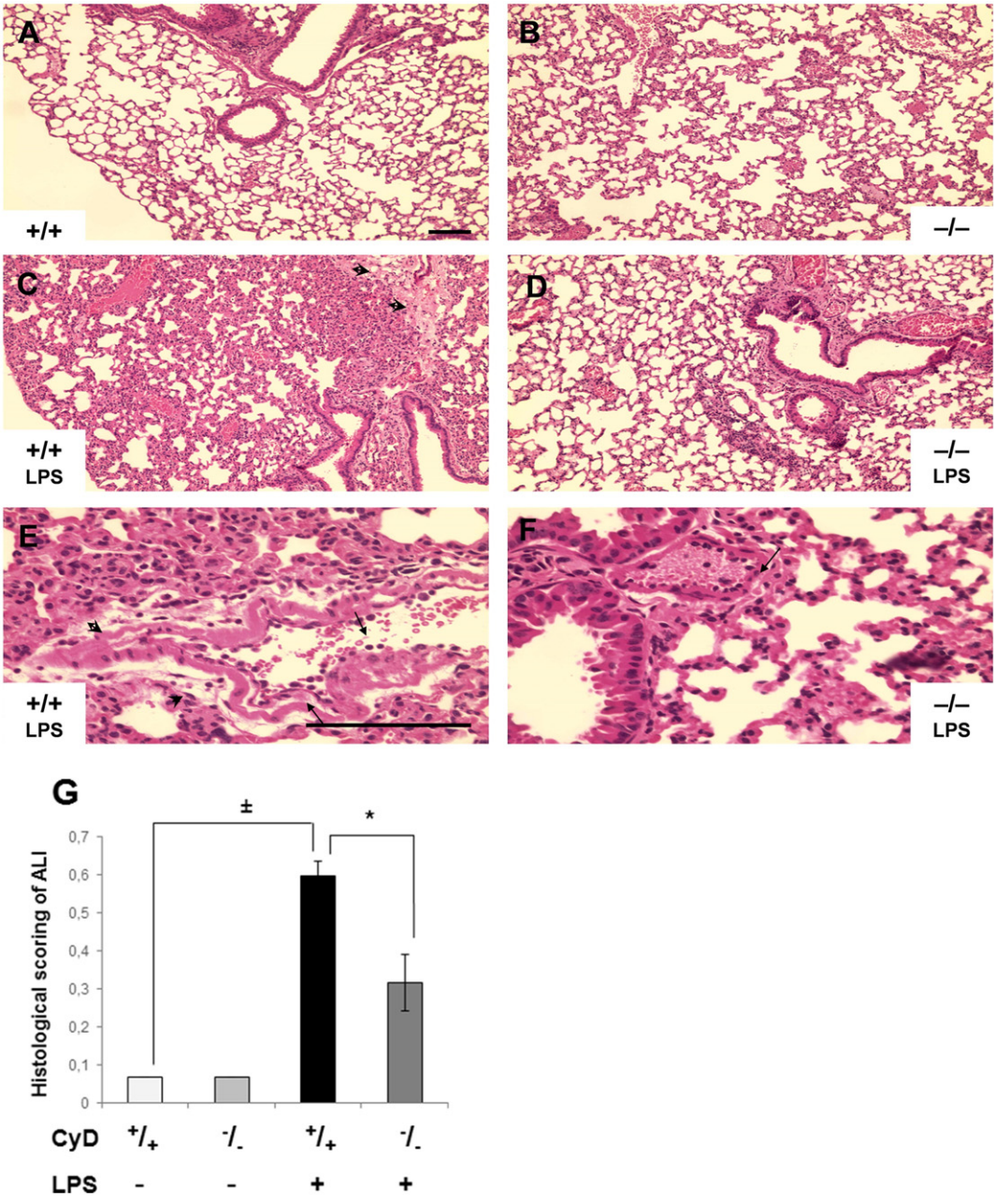

Fig. 2. Deletion of CypD prevents lung vascular permeability, edema, and inflammation induced by LPS. Representative pathological and histological analysis of lungs from untreated (A) and LPS-treated (C) wild type mice, as well as from untreated (B) and LPS-treated (D) CypD knock-out mice. Enlarged light microscopic images highlight differences of vascular events in LPS-treated wild type (E) and knock-out mice (F). Arrows pointing on marginating and transmigrating leukocytes, arrowheads indicate severe endothelial leakage with consequent perivascular edema. Original magnification was 10× (A,B,C,D) and 40× (E,F). Scale bars represent 100 μm. Histological scoring was also performed in double blinded manner according to the recommendations of the American Thoracic Society (G). Results are presented as mean ± SEM, n = 5. Significant difference between control and LPS-treated wild type animals is indicated by ±($p < 0.001$), significant difference between LPS-treated wild type and CypD knock-out animals is indicated by *($P < 0.05$).

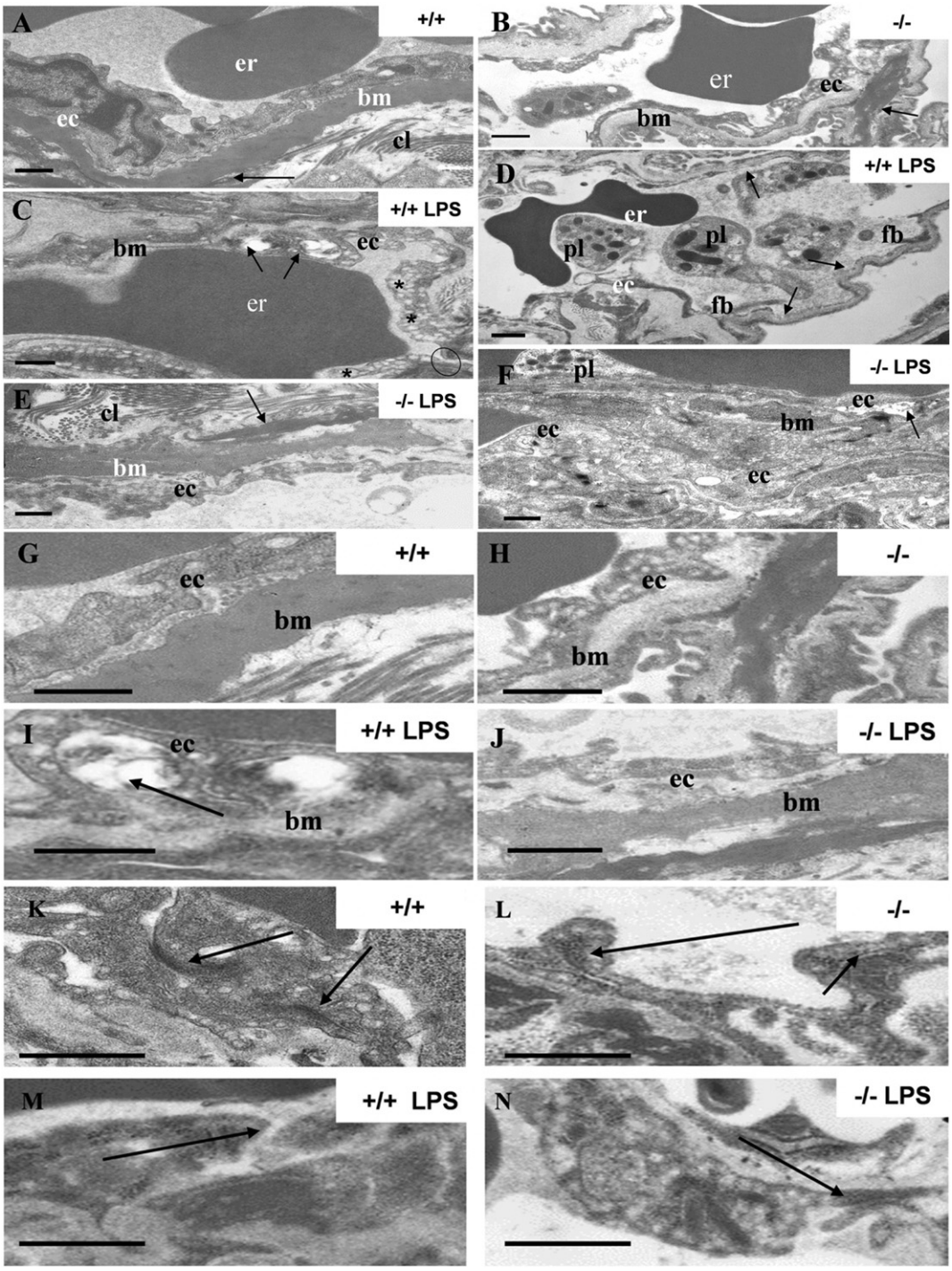

Fig. 3. Lack of CypD prevents the fine structural anatomy of lung tissue damaged by LPS. (A) In untreated wild type mice blood vessel endothelial cells (ec) attach intact basement membrane (bm). Dense layer of fibro elastic membrane supports interseptal wall (arrow). er: erythrocyte, cl: collagen fibers. (B) In CypD knock-out mice intact basement membrane (bm) and endothelial cell (ec) are visible. Prominent fibro elastic layer (arrow) lying beneath basement membrane. (C, D) LPS-treated wild type mice show seriously degenerating portion of an endothelial cell (ec) with large vacuoles appearing in cytoplasm (arrows, C) and thinner basement membrane (bm). Number and size of pinocytotic vesicles (stars) are increased, cytoplasm is swollen. Widened inter endothelial junction (circle) is also shown. Portions of endothelial cells are focally detached from basal membrane (arrows, D). Denuded patches serve potential surfaces to fine fibrin branches (fb) to attach. Blood vessel lumen is congested with platelets (pl). (E, F) In CypD knock-out LPS-treated mice the structure of blood vessel walls is almost identical with that of control animals. Intact endothelial cell (ec) basement membrane (bm) and fibro elastic membrane (arrow, E) are shown. Diffuse appearance of collagen fibers (cl) could also be observed. In some cases intact endothelial cell (ec) portions were seen focally detached (arrow, F) from basement membrane (bm). Cytoplasmic swelling could not be seen. (G, H) Fine structure of endothelial cells show no morphological changes between $CypD^{+-+}$ vs $CypD^{-/-}$. (I, J) Serious endothelial cytoplasmic degeneration is visible (arrow, I) in LPS-treated wild type compared to knock-out mice. (K, L) Dense membrane sections of inter endothelial junctions (arrows) in blood vessel walls are intact both in wild type and CypD knock-out control animals. (M, N) Arrows show widened and intact thigh junctions in blood vessel wall of LPS-treated wild type and CypD knock-out animals, respectively. Scale bars: 500 nm.

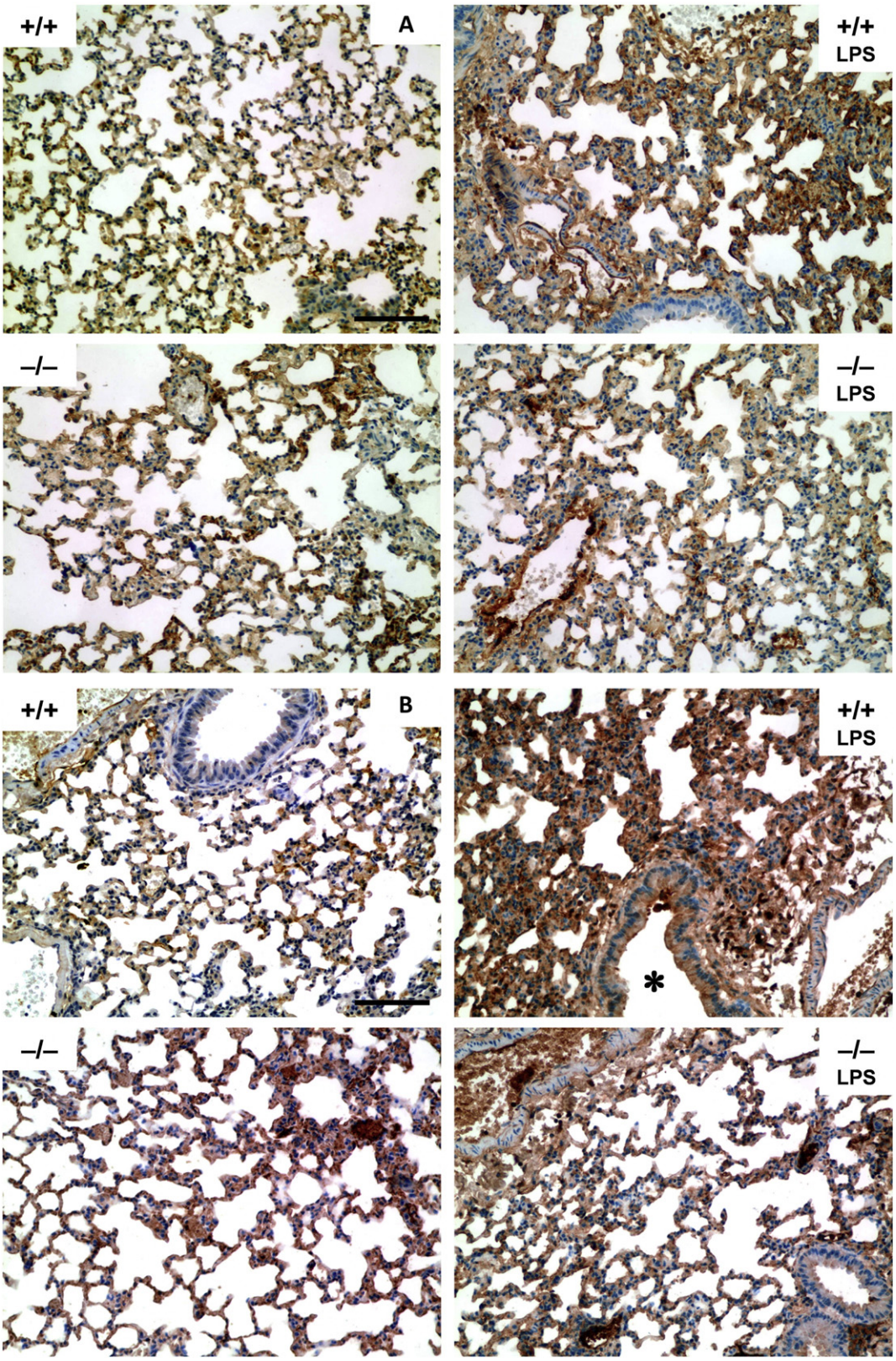

Fig. 4. Loss of CypD protects the lung epithelial cells against oxidative damage. Immunohistochemical staining of mouse lungs for nitrotyrosine (A) and for 4-hydroxy-2-noneal Michael adducts (B) in lung tissue counterstained with hematoxylin. Endothelia of lung vessels in LPS-treated wild type mice were intensively stained compared to CypD knock-out mice. Epithelial cells showed prominent positivity in wild type, but not in knock-out LPS-treated animals. Star indicates airway lumen with strong positivity of bronchial cells and secretory product. Scale bar represents 100 μm.

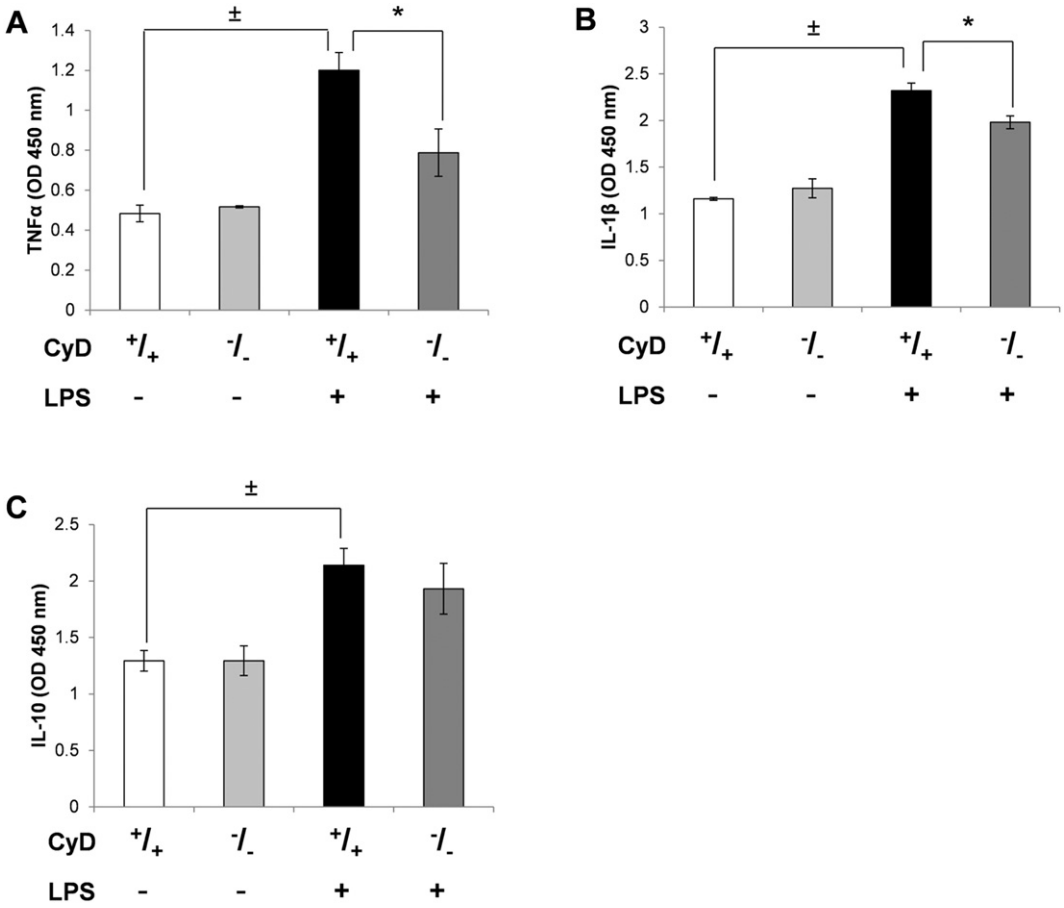

Fig. 5. Effect of LPS on cytokine production of wild type and CypD$^{-/-}$ mice. Determination of proinflammatory cytokines TNFα (A) and IL-1β (B), and anti-inflammatory cytokine IL-10 (C) 24 h after LPS-treatment from total lung homogenates by ELISA. Bars represent mean ± SEM of optical densities, n = 4. Significant difference between control and LPS-treated wild type animals is indicated by ±($p < 0.05$), significant difference between LPS-treated wild type and CypD knock-out animals is indicated by *($P < 0.05$).

3. Results

3.1. Mice lacking CypD survive lethal endotoxemia

CypD knock-out animals exhibited improved survival rate after intraperitoneal high dose LPS treatment compared to wild type mice. Out of the 8 CypD$^{-/-}$ mice two (25%) died within the first 30 h but after that no deaths occurred. However all of the 8 wild type mice died within 60 h (Fig. 1). These results show that the loss of CypD massively reduces mortality.

3.2. CypD knock-out mice are protected against LPS-induced histopathological changes

Histological examination revealed severe lung injury in LPS-treated wild type animals. On hematoxylin-eosin stained sections, alveolar wall thickening, blood vessel congestion and perivascular exudation were seen, which are suggestive of impaired tissue architecture and function, while robust interstitial neutrophil infiltration indicated ongoing immune response (Fig. 2C). Interstitial accumulation of neutrophils was markedly decreased in LPS-treated CypD$^{-/-}$ mice (Fig. 2E, 2F). Other pathological changes like alveolar widening and perivascular edema were also significantly milder in CypD$^{-/-}$ lungs and no thrombotic event could be observed despite moderate congestion (Fig. 2D). Lungs of control animals in both groups had normal tissue architecture with thin alveolar walls, occasional intra-alveolar macrophages and few neutrophils (Fig. 2A, 2B). For making histological examination quantitative a scoring was performed as described earlier (Fig. 2G). Scores were significantly higher in the LPS-treated wild type mice compared to CypD knock-outs mainly resulting from marked differences in interstitial neutrophil accumulation and alveolar thickening.

3.3. Lack of CypD prevents the fine structural anatomy of lung tissue damaged by LPS

LPS treatment induced serious lesions in the lung tissue of wild type mice. Endothelial cells were swollen loaded with cytoplasmic vacuoles and the number of pinocytotic vesicles was increased (Fig. 3C, 3I). Inter-endothelial connections of endothelial cells were damaged or dilated (Fig. 3M). An impaired, leaky endothelial layer of blood vessels allowed extravasation of intravascular fluid resulting in tissue edema. Another sign of impaired blood vessel functioning was a detached basal membrane with an unsettled fibroelastic layer in the alveolar septa (Fig. 3D). These denuded surfaces are potential targets of fibrin attachment and hyaline membrane formation. The proinflammatory activity of fibrin fragments and massive liberation of immune cell molecules may explain the appearance of a considerable amount of cell debris. Obvious thickening of the alveolar septa by accumulated connective tissue indicates strong fibrosis (Fig. 3D). Tissue organization of CypD$^{-/-}$ mice with or without LPS treatment was almost identical to that of wild type untreated animals (Fig. 3A, 3B, 3G–L). The level of septal thickening was not comparable to that in wild type LPS-treated

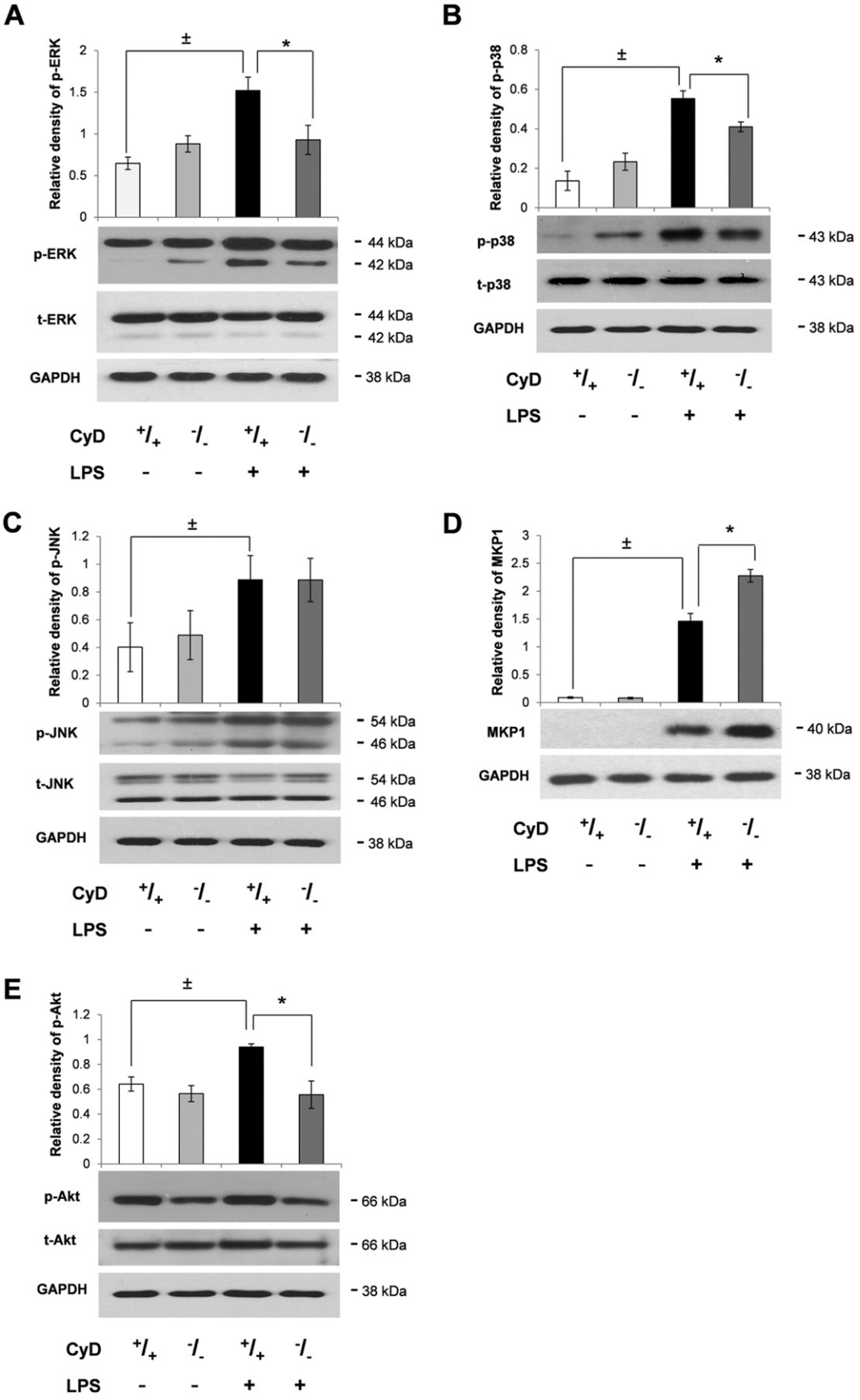

Fig. 6. Deficiency of CypD affects MAPKs, MKP-1 and Akt in mouse lungs after LPS treatment. Activation of ERK (A), p38 (B), SAPK/JNK (C), MKP-1 (D) and Akt (E) in lung total homogenates was determined 24 h after LPS treatment by immunoblotting utilizing phosphorylation specific and total primary antibodies. Total proteins (non-phosphorylated) and GAPDH were used as loading controls. A representative blot as well as a bar diagram of the quantified blots are presented. Bars represent mean ± SEM of pixel densities, n = 4. Significant difference between control and LPS-treated wild type animals is indicated by ±($p < 0.05$), significant difference between LPS-treated wild type and CypD knock-out animals is indicated by *($p < 0.05$).

animals (Fig. 3D, 3E). This observation indicates the quicker resolution of acute lung tissue lesions or much milder tissue injury.

3.4. Loss of CypD protects lung epithelial cells against oxidative damage

Lung tissue sections were examined with immunohistochemistry using antibodies against nitrotyrosine, and 4-hydroxy-2-noneal Michael adducts. LPS treatment markedly enhanced immunohistochemical staining in endothelial and lung epithelial cells of wild type animals. Endothelial and epithelial cells of CypD$^{-/-}$ mice showed less intense staining (Fig. 4A). The extensive lipid-peroxidation damage after LPS treatment in wild type animals was also visible regarding bronchial mucinosus cells. In contrast, endotoxemic CypD$^{-/-}$ mice exhibited a markedly reduced staining of endothelial tissue, while the intensity of epithelial positivity was almost the same as in wild type and knock-out animals without LPS treatment (Fig. 4B).

3.5. Absence of CypD impairs proinflammatory, but does not affect anti-inflammatory cytokine production

During ALI, early phase cytokines promote the production of chemokines by resident cells to enhance neutrophil sequestration into the lung. Clinical studies have proven the importance of these factors, since the outcome of patients with ARDS significantly correlates with the concentration of these cytokines in bronchoalveolar lavage fluid [7,21,22]. In our experiments, LPS treatment resulted in elevated TNFα and IL-1β levels, measured in lung homogenates, while the amount of these cytokines was markedly decreased in LPS-treated CypD$^{-/-}$ mice (Fig. 5A, 5B). IL-10, responsible for limiting inflammatory processes, ameliorates endotoxemia-induced ALI and high levels in the lungs of patients suffering from ARDS correlated with better outcome [23,24]. In our study, there was no difference in the amount of anti-inflammatory IL-10 in total lung homogenates between wild type and knock-out animals 24 h after LPS administration (Fig. 5C), as both increased significantly.

3.6. Deficiency of CypD affects the activation of MAPKs through MKP-1 and Akt in mouse lungs after LPS treatment

Phosphorylation and activation of MAPKs was shown to play an important role in the development of ALI following LPS exposure [25,26]. In our experiments, phosphorylation levels of extracellular signal-regulated kinase (ERK), p38, and c-Jun. N-terminal kinase (JNK) were significantly elevated 24 h after LPS treatment in wild type animals, while the activation of ERK and p38 was lower in the lungs of LPS-treated CypD$^{-/-}$ mice (Fig. 6A, B). No difference could be observed in JNK phosphorylation between knock-out and wild type animals after LPS challenge (Fig. 6C).

MAP kinases are under the direct negative regulation through dephosphatase activity of MAPK-phosphatase-1 (MKP1). The level of MKP1 was up-regulated in CypD$^{-/-}$ mice compared to wild type animals after LPS treatment (Fig. 6D).

Beside MAP kinases Akt contributes to the TLR4 signaling cascade leading to NF-κB activation and promoting inflammatory processes in the lung. In our experiment, LPS treatment significantly enhanced the phosphorylation of Akt in the lungs of wild type animals, while this effect was strongly reduced in CypD$^{-/-}$ animals, resulting in a phosphorylation level that was comparable to that seen in control animals (Fig. 6E).

3.7. CypD knock-out mice do not exhibit prominent NF-κB activation after LPS treatment

We determined the phosphorylation level of the p65 subunit of NF-κB and inhibitory-κB (IκB). LPS caused a significant activation of NF-κB in wild type mice compared to CypD$^{-/-}$ animals (Fig. 7A). Similarly, robust IκB phosphorylation was found in wild type animals after LPS treatment; however, CypD$^{-/-}$ mice showed decreased phosphorylation, which seems to confirm our data regarding NF-κB activation (Fig. 7B).

3.8. Marked differences between wild type and CypD knock-out animals regarding NF-κB-mediated gene expression

To gain further insight into the functional inhibition of NF-κB, we determined the gene expression of NF-κB-regulated inflammatory mediators that are crucial in the pathophysiology of LPS-induced ALI using qRT-PCR. Expression of CD14, CXCl2, IFNγ, TNFα, IL-1 and inducible NO synthase (iNOS) was elevated in LPS-treated wild type animals; this LPS-induced overexpression was strongly reduced in every case in the knock-out mice. Our data show that NF-κB regulation in CypD$^{-/-}$ animals is not limited to the level of phosphorylation

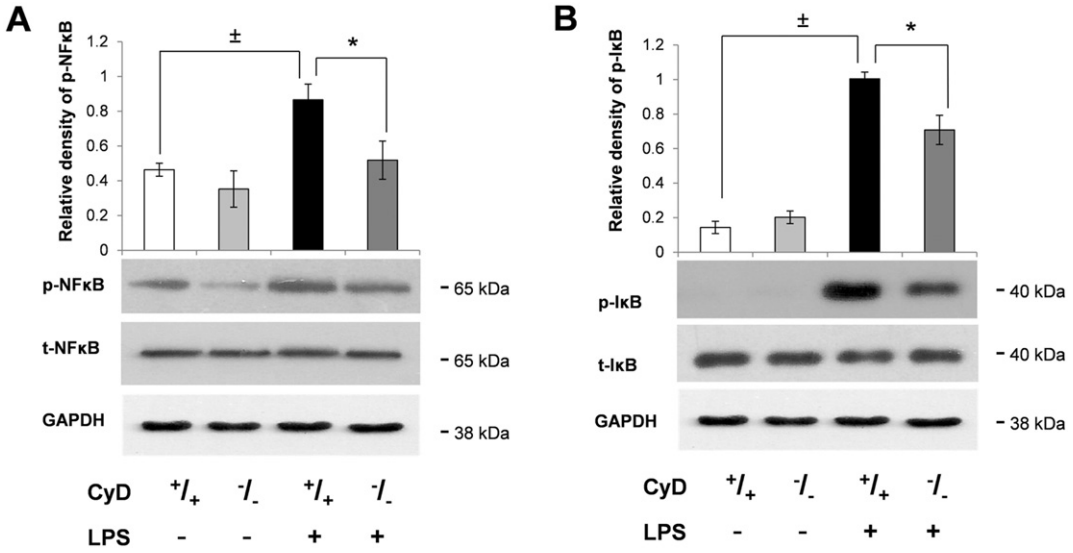

Fig. 7. CypD is required for LPS-induced NF-κB activation. Phosphorylation of NF-κB (A) and IκB (B) in lung total homogenates was determined 24 h after LPS treatment by immunoblotting, utilizing phosphorylation specific primary antibodies. Total proteins (non-phosphorylated) and GAPDH were used as loading controls. A representative blot as well as a bar diagram of the quantified blots are presented. Bars represent mean ± SEM of pixel densities, n = 4. Significant difference between control and LPS-treated wild type animals is indicated by ±($p < 0.001$), significant difference between LPS-treated wild type and CypD knock-out animals is indicated by *($P < 0.05$).

of key signaling enzymes, but it affects the transcription of the related genes as well (Fig. 8).

4. Discussion

In the present study, we demonstrated that a deficiency of CypD ameliorates pathological consequences of endotoxemia-induced ALI, both at the tissue and molecular levels, and massively reduces mortality rate. Cyclophilins are ubiquitous proteins differing in their subcellular localization and binding affinity to CsA. CsA inhibits calcineurin thereby suppresses MKP-1 expression resulting in increased MAPK activation [27]. Therefore, considering the importance of MAPKs in NF-κB activation, CsA is obviously unsuitable for studying the effect of mPT impairment on LPS-induced inflammatory response. To resolve this problem and to focus on the role of CypD and mPT on LPS-induced inflammation, we used a CypD$^{-/-}$ model.

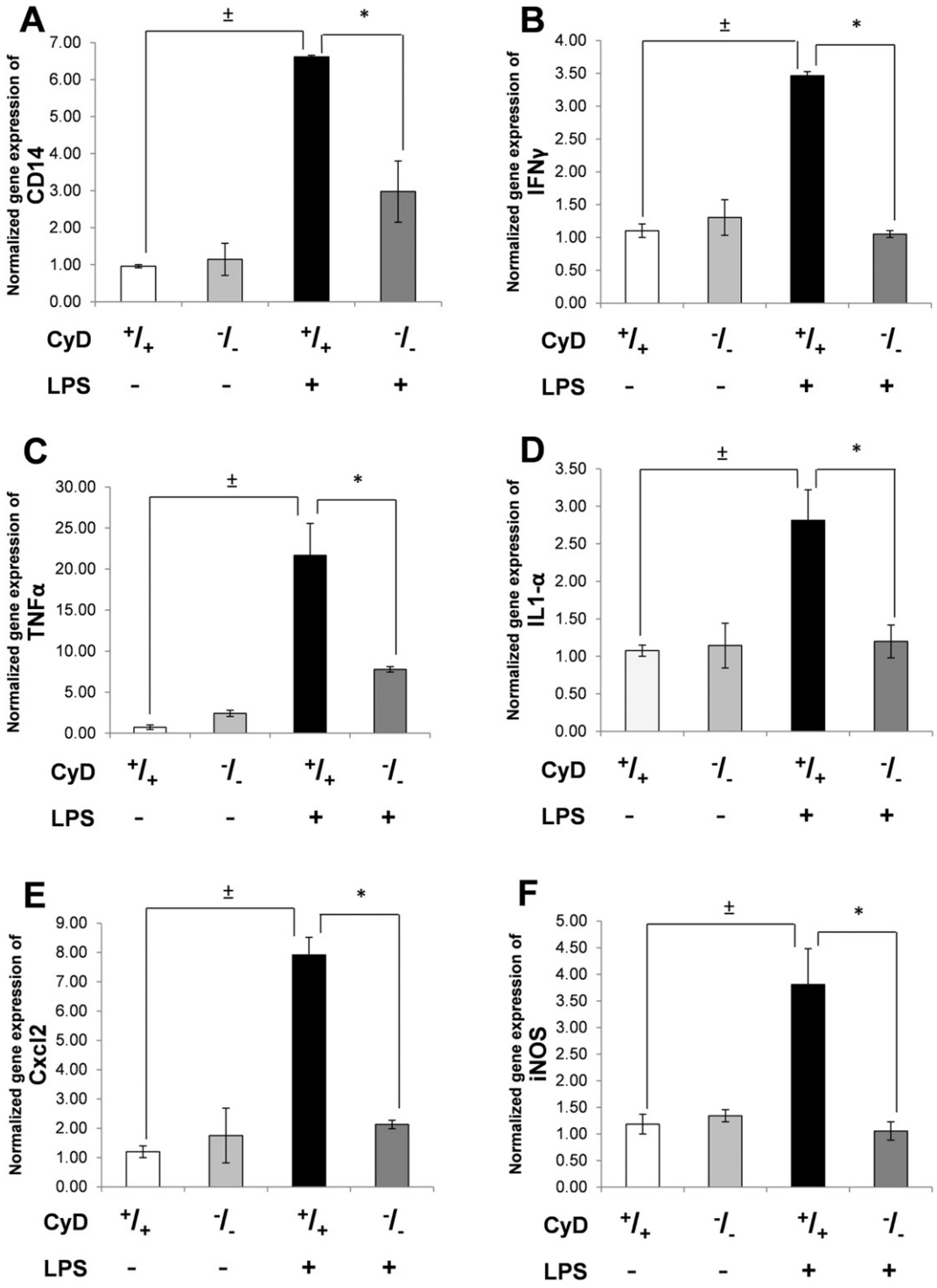

Fig. 8. CypD regulates LPS-induced NF-κB-mediated gene expression. The expression of NF-κB-mediated inflammatory genes, CD14 (A), IFN-γ (B), TNFα (C), IL-1α (D), Cxcl2 (E) and iNOS (F) was determined 24 h after LPS treatment in lung tissue by RT-PCR. Actin was used as a housekeeping gene to generate the ΔCt values. Data were normalized to ΔCt values of untreated controls. Results are presented as mean ± SEM, n = 4. Significant difference between control and LPS-treated wild type animals is indicated by ±($p < 0.001$), significant difference between LPS-treated wild type and CypD knock-out animals is indicated by *($P < 0.05$).

LPS is known to cause excessive inflammatory response with oxidant–antioxidant imbalance in many organs, severely affecting the lungs. Lung epithelial cells and macrophages, as well as sequestered neutrophils produce excessive amounts of ROS, amplifying oxidant events. Mitochondrial ROS production-induced cellular damage has been implicated in the pathophysiology of LPS-induced inflammation and ALI [28] characterized by endothelial barrier dysfunction, interstitial edema and thickening, epithelial damage, and the accumulation of neutrophils. Our histological results showed the same characteristics in the lungs of LPS-challenged wild type mice, but animals lacking CypD showed only mild tissue injury. Histological scores supported these findings. The deleterious effect of ROS on endothelial and epithelial morphology and barrier function has been demonstrated at the subcellular fine structural level using electron microscopy; however, a definitive protective effect was found in CypD-deficient mice. Our results suggest that the loss of CypD greatly diminishes ROS and RNS production after LPS treatment with the consequent attenuation of microscopic and subcellular pathological changes and oxidative tissue damage in the lungs of mice.

ROS contribute to the inflammatory phenotype, with the increased production of proinflammatory cytokines in lung cells. Elevated concentrations of proinflammatory chemokines and cytokines, including IL-8, IL-1β, and TNFα, in the lungs are critical regulators of the outcome of ALI. Compared to wild type animals, in CypD-deficient mice, the level of TNFα and IL-1β produced by resident cells was decreased, indicating that the lack of CypD could severely interfere with cytokine generation, possibly due to reduced mitochondrial ROS production. This strong correlation between mitochondrial ROS and proinflammatory cytokine production was also reported by Bulua and his coworkers, pointing to the fact that the blockade of mitochondrial ROS generation efficiently reduces inflammatory cytokine production after treatment in cells from patients with TNF receptor-associated periodic syndrome and from healthy individuals [29].

As a counterbalance, IL-10 is a key anti-inflammatory cytokine in the down-regulation of inflammatory response. One of its key functions is regulation of the pathogen-mediated activation of macrophages and dendritic cells, consequentially inhibiting the expression of chemokines, inflammatory enzymes, and potent proinflammatory cytokines. Elevated levels of IL-10 after LPS exposure did not differ in the two LPS-treated groups, indicating that the ameliorated inflammatory processes in CypD-deficient animals are not a consequence of anti-inflammatory mechanisms but of attenuated ROS production.

ROS are important chemical mediators that regulate signal transduction pathways, including members of the MAP kinases. In line with previous studies, [25,26] we found the increased phosphorylation of MAPKs in the lungs after LPS treatment. Phosphorylation of redox-sensitive p38 and ERK was markedly decreased in CypD-deficient mice; however, JNK activation was unaltered in our experiments. Although ROS could activate all three MAPKs, this regulation is conducted by different upstream regulators independently of each other. It was previously reported that H_2O_2 stimulates JNK but not p38 and ERK via a pathway that is dependent on Src; however, the exact mechanisms for ROS-mediated p38 and ERK activation remain unknown [30]. Based on our results the depletion of CypD exerts its effect on ROS-induced MAPK activation in p38- and ERK-dependent and JNK-independent ways. Besides the regulation of upstream mediators of MAPKs, direct control mechanisms could act also through MKP-1 activity. MKP-1 is a central redox sensitive regulator of ERK and p38 during endotoxemia, ameliorating monocyte activation and consequential lung injury [31,11]. Up-regulation of MKP-1 in CypD knock-out mice upon LPS exposure represents a strong protective pathway due to the attenuated activation of ERK and p38. Previous studies have shown that p38 is regulated by Akt as well, positively influencing NF-κB activation [32]. Indeed, the phosphorylation pattern of p38 followed that of Akt in our experiments. Since Akt could be activated by ROS [33] and IL-1β [32], a lack of CypD could down-regulate the Akt-p38-NF-κB pathway through these inflammatory mediators. In accordance with these findings, NF-κB and IκB phosphorylation increased dramatically after LPS treatment in the lungs of wild type but not CypD-deficient animals. Moreover, we proved the functional inhibition of NF-κB activity in the absence of CypD, analyzing NF-κB-related genes at the mRNA and protein levels. In CypD-deficient mice, the expression of important participants of TLR4 signaling (CD14, iNOS) and mediators of ALI, like chemokines and cytokines (Cxcl2, IFNγ, TNFα, IL-1α), showed a significant decrease compared to wild type animals. Our gene expression data suggest that the downregulation of NF-κB and the related genes by the lack of CypD may be essential to prevent or treat inflammatory diseases.

In summary, we demonstrate that the loss of essential mPT modulatory protein CypD can intensely ameliorate endotoxemia-induced lung injury in mice through down-regulation of the NF-κB pathway, inflammatory mediators and reducing the production of ROS. Our data highlight a previously unknown regulatory function of mitochondria due to the mediation of mPT during inflammatory responses. This finding offers a valuable therapeutic target in conditions of acute inflammation including ALI.

Conflict of interest

The authors declare no conflict of interest.

Acknowledgements

This research was supported by the European Union and the State of Hungary, co-financed by the European Social Fund in the framework of TÁMOP-4.2.4.A/2-11/1-2012-0001 'National Excellence Program'. This work was also supported by PTE ÁOK-KA-2013/31 and by OTKA K104220.

References

[1] K.L. Brigham, B. Meyrick, Endotoxin and lung injury, Am. Rev. Respir. Dis. 133 (1986) 913–927.
[2] O. Takeuchi, K. Hoshino, T. Kawai, H. Sanjo, H. Takada, et al., Differential roles of TLR2 and TLR4 in recognition of Gram-negative and Gram-positive bacterial cell wall components, Immunity 11 (1999) 443–451.
[3] Y.C. Lu, W.C. Yeh, P.S. Ohashi, LPS/TLR4 signal transduction pathway, Cytokine 42 (2008) 145–151.
[4] D. Togbe, S. Schnyder-Candrian, B. Schnyder, E. Doz, N. Noulin, et al., Toll-like receptor and tumour necrosis factor dependent endotoxin-induced acute lung injury, Int. J. Exp. Pathol. 88 (2007) 387–391.
[5] T.S. Blackwell, E.P. Holden, T.R. Blackwell, J.E. DeLarco, J.W. Christman, Cytokine-induced neutrophil chemoattractant mediates neutrophilic alveolitis in rats: association with nuclear factor kappa B activation, Am. J. Respir. Cell Mol. Biol. 11 (1994) 464–472.
[6] T.S. Blackwell, J.W. Christman, The role of nuclear factor-kappa B in cytokine gene regulation, Am. J. Respir. Cell Mol. Biol. 17 (1997) 3–9.
[7] J. Grommes, O. Soehnlein, Contribution of neutrophils to acute lung injury, Mol. Med. 17 (2011) 293–307.
[8] B. Veres, F. Gallyas Jr., G. Varbiro, Z. Berente, E. Osz, et al., Decrease of the inflammatory response and induction of the Akt/protein kinase B pathway by poly-(ADP-ribose) polymerase 1 inhibitor in endotoxin-induced septic shock, Biochem. Pharmacol. 65 (2003) 1373–1382.
[9] B. Veres, B. Radnai, F. Gallyas Jr., G. Varbiro, Z. Berente, et al., Regulation of kinase cascades and transcription factors by a poly(ADP-ribose) polymerase-1 inhibitor, 4-hydroxyquinazoline, in lipopolysaccharide-induced inflammation in mice, J. Pharmacol. Exp. Ther. 310 (2004) 247–255.
[10] P.B. Jakus, N. Kalman, C. Antus, B. Radnai, Z. Tucsek, et al., TRAF6 is functional in inhibition of TLR4-mediated NF-κB activation by resveratrol, J. Nutr. Biochem. 24 (2013) 819–823.
[11] Z. Tucsek, B. Radnai, B. Racz, B. Debreceni, J.K. Priber, et al., Suppressing LPS-induced early signal transduction in macrophages by a polyphenol degradation product: a critical role of MKP-1, J. Leukoc. Biol. 89 (2011) 105–111.
[12] M. Crompton, The mitochondrial permeability transition pore and its role in cell death, Biochem. J. 341 (1999) 233–249.
[13] V. Giorgio, S. von Stockum, M. Antoniel, A. Fabbro, F. Fogolari, et al., Dimers of mitochondrial ATP synthase form the permeability transition pore, Proc. Natl. Acad. Sci. U. S. A. 110 (2013) 5887–5892.
[14] C.P. Baines, R.A. Kaiser, N.H. Purcell, N.S. Blair, H. Osinska, et al., Loss of cyclophilin D reveals a critical role for mitochondrial permeability transition in cell death, Nature 434 (2005) 658–662.

[15] E. Basso, L. Fante, J. Fowlkes, V. Petronilli, M.A. Forte, et al., Properties of the permeability transition pore in mitochondria devoid of cyclophilin D, J. Biol. Chem. 280 (2005) 18558–18561.
[16] A.K. Camara, E.J. Lesnefsky, D.F. Stowe, Potential therapeutic benefits of strategies directed to mitochondria, Antioxid. Redox Signal. 13 (2010) 279–347.
[17] N.V. Naoumov, Cyclophilin inhibition as potential therapy for liver diseases, J. Hepatol. 61 (2014) 1166–1174.
[18] P. Nigro, G. Pompilio, M.C. Capogrossi, Cyclophilin a: a key player for human disease, Cell. Death Dis. 4 (2013), e888.
[19] K. Jeong, H. Kim, K. Kim, S.J. Kim, B.S. Hahn, et al., Cyclophilin B is involved in p300-mediated degradation of CHOP in tumor cell adaptation to hypoxia, Cell Death Differ. 21 (2014) 438–450.
[20] B. Fiedler, K.C. Wollert, Interference of antihypertrophic molecules and signaling pathways with the Ca^{2+}-calcineurin-NFAT cascade in cardiac myocytes, Cardiovasc. Res. 63 (2004) 450–457.
[21] G. Matute-Bello, G. Downey, B.B. Moore, S.D. Groshong, M.A. Matthay, et al., An official American thoracic society workshop report: features and measurements of experimental acute lung injury in animals, Am. J. Respir. Cell Mol. Biol. 44 (2011) 725–738.
[22] G.U. Meduri, G. Kohler, S. Headley, E. Tolley, F. Stentz, et al., Inflammatory cytokines in the BAL of patients with ARDS Persistent elevation over time predicts poor outcome, Chest 108 (1995) 1303–1314.
[23] S.C. Donnelly, R.M. Strieter, P.T. Reid, S.L. Kunkel, M.D. Burdick, et al., The association between mortality rates and decreased concentrations of interleukin-10 and interleukin-1 receptor antagonist in the lung fluids of patients with the adult respiratory distress syndrome, Ann. Intern. Med. 125 (1996) 191–196.
[24] C.L. Wu, L.Y. Lin, J.S. Yang, M.C. Chan, C.M. Hsueh, Attenuation of lipopolysaccharide-induced acute lung injury by treatment with IL-10, Respirology 14 (2009) 511–521.
[25] S. Bozinovski, J.E. Jones, R. Vlahos, J.A. Hamilton, G.P. Anderson, Granulocyte/macrophage-colony-stimulating factor (GM-CSF) regulates lung innate immunity to lipopolysaccharide through Akt/Erk activation of NFkappa B and AP-1 in vivo, J. Biol. Chem. 277 (2002) 42808–42814.
[26] H.J. Kim, H.S. Lee, Y.H. Chong, J.L. Kang, p38 mitogen-activated protein kinase up-regulates LPS-induced NF-kappaB activation in the development of lung injury and RAW 264.7 macrophages, Toxicology 225 (2006) 36–47.
[27] H.W. Lim, L. New, J. Han, J.D. Molkentin, Calcineurin enhances MAPK phosphatase-1 expression and p38 MAPK inactivation in cardiac myocytes, J. Biol. Chem. 276 (2001) 15913–15919.
[28] C. Richter, V. Gogvadze, R. Laffranchi, R. Schlapbach, M. Schweizer, et al., Oxidants in mitochondria: from physiology to diseases, Biochim. Biophys. Acta 1271 (1995) 67–74.
[29] A.C. Bulua, A. Simon, R. Maddipati, M. Pelletier, H. Park, et al., Mitochondrial reactive oxygen species promote production of proinflammatory cytokines and are elevated in TNFR1-associated periodic syndrome (TRAPS), J. Exp. Med. 208 (2011) 519–533.
[30] M. Yoshizumi, J. Abe, J. Haendeler, Q. Huang, B.C. Berk, Src and Cas mediate JNK activation but not ERK1/2 and p38 kinases by reactive oxygen species, J. Biol. Chem. 275 (2000) 11706–11712.
[31] H.S. Kim, S.L. Ullevig, D. Zamora, C.F. Lee, R. Asmis, Redox regulation of MAPK phosphatase 1 controls monocyte migration and macrophage recruitment, Proc. Natl. Acad. Sci. U. S. A. 109 (2012) E2803–E2812.
[32] L.V. Madrid, M.W. Mayo, J.Y. Reuther, A.S. Baldwin Jr., Akt stimulates the transactivation potential of the RelA/p65 subunit of NF-kappa B through utilization of the ikappa B kinase and activation of the mitogen-activated protein kinase p38, J. Biol. Chem. 276 (2001) 18934–18940.
[33] S.R. Lee, K.S. Yang, J. Kwon, C. Lee, W. Jeong, et al., Reversible inactivation of the tumor suppressor PTEN by H2O2, J. Biol. Chem. 277 (2002) 20336–20342.